2,2′:6′,2″-Terpyridine (terpy) acting as a Fluxional Bidentate Ligand. Part 4.[1] *cis*-[M(C_6F_5)$_2$(terpy)] (M = Pd or Pt): Nuclear Magnetic Resonance Studies of their Solution Dynamics and Crystal Structure of *cis*-[Pd(C_6F_5)$_2$(terpy)]†

Edward W. Abel,[a] Keith G. Orrell,*[,a] Anthony G. Osborne,[a] Helen M. Pain,[a] Vladimir Šik,[a] Michael B. Hursthouse[b] and K. M. Abdul Malik[b]

[a] *Department of Chemistry, The University, Exeter EX4 4QD, UK*

[b] *School of Chemistry and Applied Chemistry, University of Wales, College of Cardiff, Cardiff CF1 3TB, UK*

2,2′:6′,2″-Terpyridine reacted with *trans*-[M(C_6F_5)$_2$(diox)$_2$] (M = Pd or Pt, diox = 1,4-dioxane) to form the square-planar complexes *cis*-[M(C_6F_5)$_2$(terpy)] in which the terpyridine acts as a bidentate chelate ligand. In solution these complexes are fluxional with the terpyridine oscillating between equivalent bidentate modes by a mechanism consisting of a 'tick-tock' twist of the metal moiety through an angle equal to the N–M–N angle of the metal centre. Rates of this fluxion were measured by NMR spectroscopy from the exchange effects on the ^{1}H signals of the aromatic hydrogens and in the ^{19}F signals of two C_6F_5 groups. The $\Delta G^{\ddagger}$ values for the fluxion were *ca.* 71 and 94 kJ mol^{-1} for the complexes of Pd^{II} and Pt^{II} respectively. At below-ambient temperatures further changes in the ^{19}F NMR spectra of both complexes were interpreted in terms of varying rates of rotation of the unco-ordinated pyridine ring, with the rates of rotation of the C_6F_5 rings being substantially slower at all temperatures and not separately measurable. The lowest-temperature spectra suggested the presence of a pair of degenerate rotamers each having the planes of both C_6F_5 rings and the unco-ordinated pyridine ring closely parallel and orthogonal to the remainder of the ligand ring system. The crystal structure of [Pd(C_6F_5)$_2$(terpy)] confirms the bidentate chelate bonding of terpy with a N–Pd–N angle of 77.9°, and the pendant ring oriented at an angle of 46° to the adjacent co-ordinated ring.

If suitable co-ordination sites are available on a metal the heterocyclic molecule 2,2′:6′,2″-terpyridine (terpy) usually bonds as a terdentate chelate ligand.[2] If however the metal is already bound to ligands of widely differing kinetic lability the possibility arises that fewer than the three nitrogen atoms of the terpy may bond to it. This concept has recently been demonstrated in octahedral complexes with Ru^{II},[1] Re^{I},[3] Pt^{IV} (ref. 4) and W^0 (ref. 1) in which terpy is forced to act in a bidentate chelate mode. For such complexes it was shown that in solution the terpy was undergoing an oscillatory fluxional motion between equivalent bidentate bonding modes.

In this paper we explore the properties of terpy acting as a bidentate chelate ligand towards other metals and in other co-ordination geometries. Its reactions were investigated with the compounds *trans*-[M(C_6F_5)$_2$(diox)$_2$] (M = Pd^{II} or Pt^{II}, diox = 1,4-dioxane)[5,6] in the expectation that the weakly bound 1,4-dioxane molecules would be readily displaced and four-co-ordinate square-planar metal complexes involving bidentate chelate terpy would be isolated. The preparation of *cis*-[M(C_6F_5)$_2$(terpy)] (M = Pd or Pt), solution ^{1}H and ^{19}F NMR studies of the dynamic stereochemistry of the complexes, and the crystal structure of *cis*-[Pd(C_6F_5)$_2$(terpy)] are described.

Experimental

Materials.—The compounds *trans*-[M(C_6F_5)$_2$(diox)$_2$] (M = Pd or Pt) were prepared by previous methods.[5,6] 2,2′:6′,6″-Terpyridine was obtained from Aldrich.

† *Supplementary data available:* see Instructions for Authors, *J. Chem. Soc., Dalton Trans.*, 1994, Issue 1, pp. xxiii–xxviii.

Synthesis of Complexes.—All preparations were carried out using standard Schlenk techniques[7] under purified nitrogen using freshly distilled, dried and degassed solvents.

cis-*Bis(pentafluorophenyl)*(2,2′:6′,2″-*terpyridyl*)*palladium*(II). The compound *trans*-[Pd(C_6F_5)$_2$(diox)$_2$] (0.20 g, 0.32 mmol) was dissolved in diethyl ether–dichloromethane (5 cm^3:5 cm^3). Terpyridine (0.08 g, 0.34 mmol) was added to the pale yellow solution which immediately turned cloudy. The mixture was stirred at room temperature for 10 min and then filtered. The solution was concentrated under vacuum and addition of hexane (10 cm^3) yielded an off-white solid. This was washed with hexane (2 × 10 cm^3), dried under vacuum and then recrystallised twice, first from acetone by slow evaporation and then from methanol at −20 °C. Yield 0.1 g (46%).

cis-*Bis(pentafluorophenyl)*(2,2′:6′,2″-*terpyridyl*)*platinum*(II). The compound *trans*-[Pt(C_6F_5)$_2$(diox)$_2$] (0.2 g, 0.28 mmol) was dissolved in diethyl ether–dichloromethane (10 cm^3:5 cm^3). Terpyridine (0.07 g, 0.03 mmol) was added to the solution which immediately turned cloudy. The mixture was stirred at room temperature for 2 h, then the yellow solution was filtered and concentrated under reduced pressure, followed by addition of hexane (10 cm^3) to produce a pale yellow solid. The product was washed with hexane (3 × 10 cm^3) and recrystallised from dichloromethane–hexane (1:1) by slow evaporation. Yield 0.07 g (33%).

Physical Methods.—Hydrogen-1 NMR spectra were recorded on a Bruker AM250 or AC300 spectrometer operating at 250.13 or 300.13 MHz respectively, ^{13}C and ^{19}F NMR spectra on a Bruker AC300 spectrometer operating at 75.47 MHz and on a AM250 spectrometer operating at 235.32 MHz respectively. A standard B-VT 1000 variable-temperature unit was used to control the probe temperature, the calibration of this unit being

Table 1 Synthetic and analytical data for the complexes $[M(C_6F_5)_2(terpy)]$ (M = Pd or Pt)

Complex	M.p.[a]/°C	Yield[b] (%)	$\tilde{\nu}$(M–C)[c]/cm^{-1}	Analysis[d] (%) C	H	N
$[Pd(C_6F_5)_2(terpy)]$	268–270	46	799m, 771vs	48.1 (48.1)	1.7 (1.7)	6.1 (6.2)
$[Pt(C_6F_5)_2(terpy)]$	250–252	33	804m, 770vs	42.8 (42.5)	1.6 (1.5)	5.0 (5.5)

[a] With decomposition. [b] Yield quoted relative to metal-containing reactant. [c] Recorded as CsI discs; m = medium, vs = very strong. [d] Calculated values in parentheses.

checked periodically against a Comark digital thermometer. The temperatures are considered accurate to ± 1 °C. Rate data were based on bandshape analysis of ^1H or ^{19}F NMR spectra using the authors' version of the standard DNMR program,[8] and activation parameters based on experimental rate data were calculated using the THERMO program.[9] Infrared spectra were recorded as CsI discs using a Nicolet Magna 550 spectrometer, calibrated from the signal of polystyrene at 1602 cm^{-1}. Elemental analyses were performed by Butterworth Laboratories, Teddington, Middlesex.

Crystal Structure Determination of $[Pd(C_6F_5)_2(terpy)]$.—*Crystal data.* $C_{27}H_{11}F_{10}N_3Pd$, M = 673.79, triclinic, space group $P\bar{1}$, a = 7.736(7), b = 12.392(4), c = 12.978(4) Å, α = 95.34(2), β = 103.14(1), γ = 99.67(4)°, U = 1183.0(11) Å^3, Z = 2, D_c = 1.891 Mg m^{-3}, $F(000)$ = 660, Mo-Kα radiation (λ = 0.710 69 Å), μ(Mo-Kα) = 8.81 cm^{-1}.

Data collection and processing. Data were collected using a FAST TV area detector diffractometer situated at the window of a rotating-anode generator operating at 50 kV, 55 mA with a molybdenum anode as described previously.[10] Somewhat more than one hemisphere of data was collected for which 4097 reflections were recorded giving 3476 independent reflections.

Structure analysis and refinement. The structure was solved by direct methods. Full-matrix least-squares analyses were performed with non-hydrogen atoms assigned anisotropic thermal parameters. Hydrogen atoms were allowed to ride on their parent carbon atoms in the calculated position (C–H 0.96 Å). The final R and R' (unit weights) were 0.0354 and 0.0622 respectively for the 381 variables. The computer programs used are given in ref. 11.

Additional material available from the Cambridge Crystallographic Data Centre comprises H-atom coordinates, thermal parameters and remaining bond angles.

Results and Discussion

Moderate yields of the complexes *cis*-$[M(C_6F_5)_2(terpy)]$ (M = Pd or Pt) as air-stable crystalline solids were obtained. They were characterised by elemental analysis, ^1H and ^{19}F NMR studies (see later), and by infrared spectroscopy where two peaks assignable to mainly M–C stretching vibrations[12,13] indicated a *cis* geometry for the two C_6F_5 groups (Table 1).

Solution-state NMR Spectroscopy.—(*a*) *Ambient-temperature studies.* ^1H *NMR spectra.* The room-temperature spectrum of the palladium(II) complex consisted of a number of broad bands. However, these sharpened on cooling to 0 °C to give a well resolved spectrum which was fully assigned by selective-decoupling experiments. The spectrum is shown in Fig. 1. The eleven chemical shifts (Table 2) are clearly associated with a bidentate terpy complex. The spectrum is almost first order with the exception of the signals due to hydrogens H_J, H_K and H_L of the central pyridine ring. These constitute an ABX system with the shifts of H_J and H_K being almost identical (*i.e.* an AA'X system).[14] These hydrogens form a composite pair and their combined signal shows coupling to H_L, while the latter displays

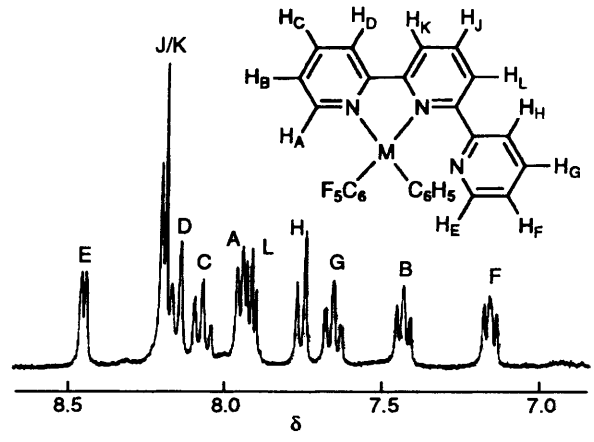

Fig. 1 The 300 MHz ^1H NMR spectrum of *cis*-$[Pd(C_6F_5)_2(terpy)]$ in $(CDCl_2)_2$ at 0 °C

virtual coupling to both H_J and H_K. The doublet and triplet splittings of these signals do not represent pure scalar couplings and the magnitudes of $J(H_JH_K)$ and $J(H_JH_L)$ given in Table 3 are estimates. One notable point in the signal assignments is that the highest-frequency doublet is assigned to H_E in contrast to previous terpy complexes when the highest-frequency signal was assigned to the hydrogen adjacent to the *co-ordinated* nitrogen of the outer ring, namely H_A. However, in this complex, the H_A hydrogen resides well within a shielding zone of the adjacent pentafluorophenyl ring and thus resonates at an appreciably lower frequency than those observed for the complexes of Ru^{II},[1] Mo^0,[1] W^0 (ref. 1) and Re^I.[3] The hydrogens H_B, H_C and H_D are largely unaffected by this ring-current effect but are influenced by the usual deshielding accompanying co-ordination. This leads to high-frequency co-ordination shifts for H_B and H_C and a low-frequency shift for H_D.

The ambient-temperature spectrum of the platinum(II) complex was assigned in a similar way. The shifts were measured at 70 °C (Table 2) where the spectral resolution was somewhat higher than at ambient temperatures.

^{19}F *NMR spectra.* The spectra of both complexes revealed six distinct fluorine environments associated with the *ortho*, *meta* and *para* positions of the two non-equivalent C_6F_5 rings. The *o*-fluorine signals exhibited a large high-frequency shift (*ca.* 40 ppm) relative to C_6F_6, used as a reference material, whereas the *m*- and *p*-fluorine signals showed very small co-ordination shifts (Table 4). The assignment of the two sets of ^{19}F signals to the two C_6F_5 rings (labelled A and B) was made by a ^{19}F correlation spectroscopy (COSY) experiment. Scalar coupling cross-peaks showed that the higher-frequency *ortho* signal was coupled to the lower-frequency partners of the *meta* and *para* signal pairs. The spectrum of the palladium(II) complex at 30 °C (Fig. 2) is assigned accordingly. Unfortunately it did not prove possible to identify the individual C_6F_5 rings in the structures of the two complexes. In principle, this should be possible if ^1H–^{19}F nuclear Overhauser effect (NOE) difference or hetero-

Table 2 Proton NMR chemical shift data* for 2,2′:6′,2″-terpyridine and the complexes *cis*-$[M(C_6F_5)_2(terpy)]$ (M = Pd or Pt)

			δ					
Compound	Solvent	T/°C	H_A, H_E	H_B, H_F	H_C, H_G	H_D, H_H	H_J	H_K, H_L
Terpyridine	CD_2Cl_2	30	8.69	7.30	7.83	8.61	7.94	8.45
$[Pd(C_6F_5)_2(terpy)]$	$(CDCl_2)_2$	0	7.95(H_A)	7.43(H_B)	8.07(H_C)	8.15(H_D)	8.19	8.19(H_K)
			8.45(H_E)	7.16(H_F)	7.65(H_G)	7.76(H_H)		7.91(H_L)
$[Pt(C_6F_5)_2(terpy)]$	$(CDCl_2)_2$	70	8.02(H_A)	7.47(H_B)	8.18(H_C)	8.19(H_D)	8.27	8.36(H_K)
			8.47(H_E)	7.15(H_F)	7.65(H_G)	7.91(H_H)		8.16(H_L)

* Relative to $SiMe_4$ (δ 0), recorded at 300 MHz, see Fig. 1 for hydrogen labelling.

Table 3 Proton NMR scalar coupling constant data (in Hz) for the complexes $[M(C_6F_5)_2(terpy)]$ (M = Pd or Pt)

J	$[Pd(C_6F_5)_2(terpy)]$	$[Pt(C_6F_5)_2(terpy)]$
$J(H_AH_B)$, $J(H_EH_F)$	5.3, 4.6	5.5, 4.4
$J(H_AH_C)$, $J(H_EH_G)$	*, 1.6	2.0, 2.0
$J(H_BH_C)$, $J(H_FH_G)$	7.5, 7.8	7.6, 7.0
$J(H_CH_D)$, $J(H_GH_H)$	8.0, 7.9	8.0, 8.0
$J(H_JH_K)$, $J(H_JH_L)$	8.0, 8.0	8.1, 8.1

* Not measured accurately; $J(H_KH_L)$ not measured.

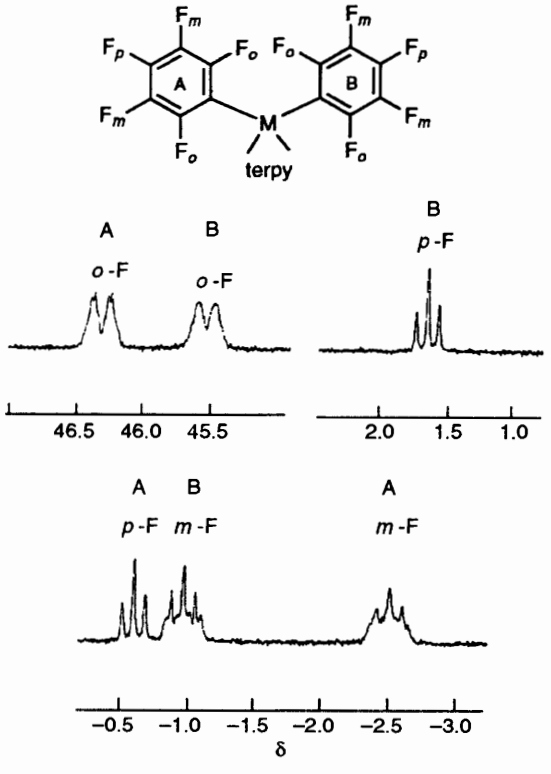

Fig. 2 The ^{19}F NMR spectrum of *cis*-$[Pd(C_6F_5)_2(terpy)]$ in $(CDCl_2)_2$ at 30 °C

nuclear two-dimensional NOESY[15] experiments could be performed to identify any cross-relaxation between the hydrogens of the pendant pyridine ring and the fluorines of the adjacent pentafluorophenyl ring. However, such heteronuclear one- and two-dimensional experiments were not available to us because of the absence of separate ^1H and ^{19}F channels on our spectrometers. The ^{19}F signals in these spectra consisted of multiplet splittings primarily due to three-bond scalar couplings with adjacent ring fluorines (Table 5). The *ortho* and *meta* signals, in particular, exhibited further partially resolved splittings due to four- and five-bond cross-ring couplings. In the spectrum of the platinum(II) complex the *o*-fluorines also exhibited $^3J(^{195}Pt–^{19}F)$ couplings (Table 5). The values compare favourably with other reported values for *cis*-$Pt(C_6F_5)_2$ moieties.[16,17]

(*b*) *Above-ambient temperature studies.* ^1H *NMR spectra.* On raising the temperature of a $(CDCl_2)_2$ solution of $[Pd(C_6F_5)_2(terpy)]$ from 0 to *ca.* 140 °C the ^1H NMR spectra underwent extensive changes characteristic of the previously reported fluxional process associated with bidentate terpy complexes.[1,3,4,18] This is illustrated in Scheme 1 where the exchange interconverts the pyridyl hydrogens according to the schemes ABCD ⇌ EFGH and JKL ⇌ JLK. The 4-position hydrogen, J of the central ring is not affected by the fluxion and its signal remains sharp at all temperatures. Spectra in the range 0–120 °C are shown in Fig. 3. At 140 °C the hydrogen exchanges were rapid on the ^1H NMR time-scale and a simplified spectrum with only six chemical shifts was observed. Spectra were reversible with respect to temperature although some decomposition was apparent at temperatures above 100 °C.

The ^1H NMR spectra of a $(CDCl_2)_2$ solution of $[Pt(C_6F_5)_2(terpy)]$ were essentially unchanged up to *ca.* 100 °C. Above that temperature slight signal broadenings were detected, attributed to the onset of the fluxional shift. However, attempts to record spectra at temperatures above *ca.* 140 °C [the high-temperature limit of $(CDCl_2)_2$] failed owing to instability of the complex in higher-boiling solvents (*e.g.* hexachloroacetone).

Bandshape analyses were performed on the most suitable signals in the ^1H NMR spectra of both metal complexes. In the case of Pd^{II} the coalescence of the H_B and H_F signals was computed, allowing for three-bond scalar couplings in the analysis, and 'best-fit' rate constants obtained (Fig. 3). For Pt^{II} the fittings of the H_B and H_F signals were restricted to the high-temperature range 100–140 °C, and because the coalescence temperature was not reached the rate data are somewhat less accurate.

^{19}F *NMR spectra.* The ^{19}F NMR spectra of the palladium(II) complex were recorded in the range 30–120 °C. On raising the temperature all signals broadened extensively in accordance with exchange between the *o*-, *m*- and *p*-F signals of the two C_6F_5 rings (A and B) (Fig. 4). Coalescence temperatures for the *ortho*, *meta* and *para* signals were *ca.* 75, 90 and 100 °C respectively. In the limiting high-temperature spectrum (120 °C) three averaged chemical shifts were observed (Table 4) consistent with rapid C_6F_5 ring equivalence. Unfortunately, extensive decomposition of the complex was also evident (Fig. 4).

Above-ambient-temperature ^{19}F NMR spectra of the platinum(II) complex were not recorded on account of the very limited changes observed in the corresponding ^1H spectrum. Rates of the fluxional shift process were extracted from ^{19}F spectra of the palladium(II) complex by fitting the exchanging *o*-fluorine signals of the A and B C_6F_5 rings. The computer fittings allowed for the main three-bond *ortho–meta* scalar couplings, the weaker four- and five-bond couplings being allowed for in the choice of the effective transverse relaxation time, T_2*, of the nuclei. A good set of simulated bandshapes was obtained for spectra recorded between 50 and 110 °C (Fig. 4), and activation-energy parameters derived.

Table 4 Fluorine-19 chemical shift data[a] for the complexes $[M(C_6F_5)_2(terpy)]$ (M = Pd or Pt) at various temperatures

		δ(^{19}F)					
Complex	T/°C	*o*-F		*m*-F		*p*-F	
$[Pd(C_6F_5)_2(terpy)]$[b]	120	46.32(AB)[c]		−2.12(AB)[c]		0.04(AB)[c]	
	30	46.76(A)	45.96(B)	−1.27(B)	−2.61(A)	1.18(B)	−0.72(A)
	−50	46.79(A)	45.78(B)	−0.47(B)	−1.86(A)	1.60(B)	−0.22(A)
		46.52(A)	45.56(B)	−0.71(B)	−2.32(A)		
$[Pt(C_6F_5)_2(terpy)]$[b]	30	43.51(A)	42.75(B)	−2.40(B)	−3.45(A)	0.05(B)	−1.95(A)
	−70	43.2(A)	42.1(B)	−0.85 to −1.3(B)[d]	−2.40(A)	0.66(B)	−1.27(A)
		42.9(A)	41.5(B)		−3.10(A)		

[a] Relative to C_6F_6(δ 0); rings labelled according to Fig. 2. [b] Recorded in CD_2Cl_2 except where otherwise stated. [c] Recorded in $(CDCl_2)_2$. [d] Broad overlapping signals.

Table 5 Fluorine-19 NMR spin–spin coupling constants (in Hz) for $[M(C_6F_5)_2(terpy)]$ (M = Pd or Pt)

	Ring A		Ring B	
Complex	$\lvert J\rvert_{o,m}$	$\lvert J\rvert_{m,p}$	$\lvert J\rvert_{o,m}$	$\lvert J\rvert_{m,p}$
$[Pd(C_6F_5)_2(terpy)]$	30.0	20.6	32.2	20.3
$[Pt(C_6F_5)_2(terpy)]$	25.2[a]	20.5	30.6[b]	19.5

[a] $^3J(^{195}Pt-^{19}F)$ = 410 Hz. [b] $^3J(^{195}Pt-^{19}F)$ = 425 Hz.

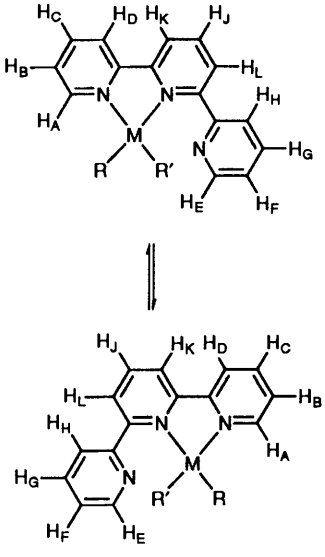

Scheme 1 Interconverting structures of the complexes $[M(C_6F_5)_2(terpy)]$ as a result of the 1,4-metallotropic shift

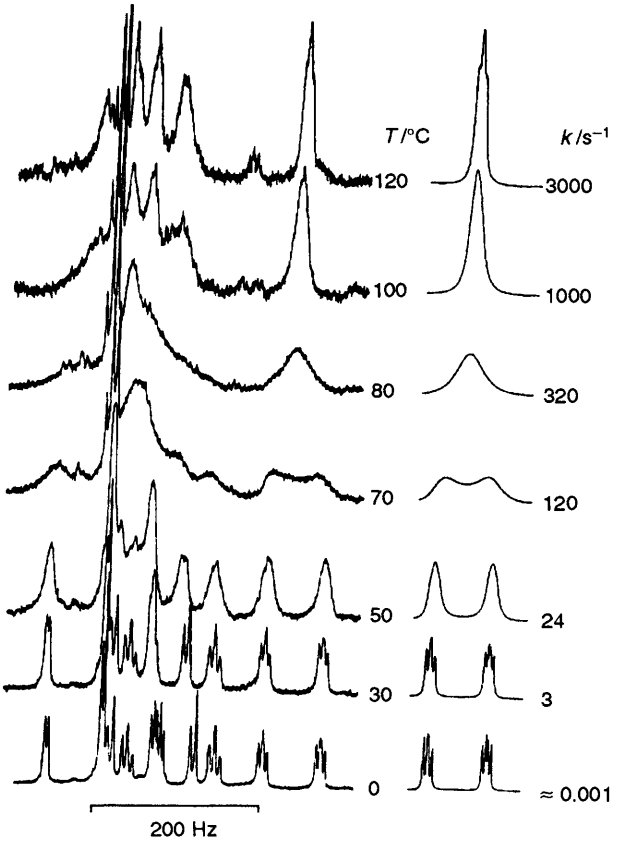

Fig. 3 The 300 MHz ^{1}H NMR spectra of $[Pd(C_6F_5)_2(terpy)]$ in $(CDCl_2)_2$ in the temperature range 0–120 °C. Computer-simulated spectra of signals B and F are shown on the right with the 'best-fit' rate constants for the fluxional process

Energies and mechanism of the fluxional process. The activation parameters for the M–N fluxion are collected in Table 6. It will be noted that energies, expressed either as $\Delta H^{\ddagger}$ or $\Delta G^{\ddagger}$ values, are relatively high with the barrier for the platinum(II) complex being *ca.* 20 kJ mol^{-1} higher than for the palladium(II) complex. This is in accordance with the relative activation energies found for these two metals both in other metal–nitrogen commutations [19] and in pyramidal inversions of metal-co-ordinated chalcogens.[20]

In the case of the present palladium(II) complex, the energy data calculated both from the pyridyl-ring hydrogen exchanges and the pentafluorophenyl exchanges are in very close agreement (Table 6), strongly suggesting that both spectral changes are the result of the same fluxional process. This conclusion was expected from our previous studies of bidentate chelate terpy complexes of Ru^{II},[1] Mo^0,[1] W^0,[1] Re^I (ref. 3) and Pt^{IV} (ref. 4) where the process was shown to involve a 'tick-tock' twist of the metal moiety relative to the terpy ligand causing an exchange of any ligands/groups in the equatorial positions. In the present case the two C_6F_5 rings of the square-planar complexes may be equated to the equatorial groups of the analogous octahedral complexes. Exchange of the two C_6F_5 rings occurring in conjunction with the ligand-exchange process thus provides unequivocal evidence that an analogous twist mechanism is operating in the present square-planar metal complexes. This mechanism is considered to proceed *via* a five-co-ordinate metal(II) intermediate in which all three heterocyclic nitrogen atoms are associated with the metal (Scheme 2).

Relative rates and energies of this fluxional process, which involves the breaking and making of two M–N bonds, range very widely according to the nature of the metal moiety. At ambient temperatures the process is fast on the ^{1}H chemical shift time-scale for $Mo(CO)_4$ and $W(CO)_4$ ($\Delta G^{\ddagger}$ = 48 and 56 kJ mol^{-1}), is of intermediate rate for $PtXMe_3$ (X = halide) ($\Delta G^{\ddagger} \approx 62$ kJ mol^{-1}) and is limitingly slow for $Pd(C_6F_5)_2$, $ReX(CO)_3$, $RuX_2(CO)_2$ (X = halide) and $Pt(C_6F_5)_2$ where $\Delta G^{\ddagger}$ values range from 71 to 94 kJ mol^{-1}. This order of energies is not easy to rationalise, and it must reflect differences in the electronic nature of the M–N bonds and steric requirements of

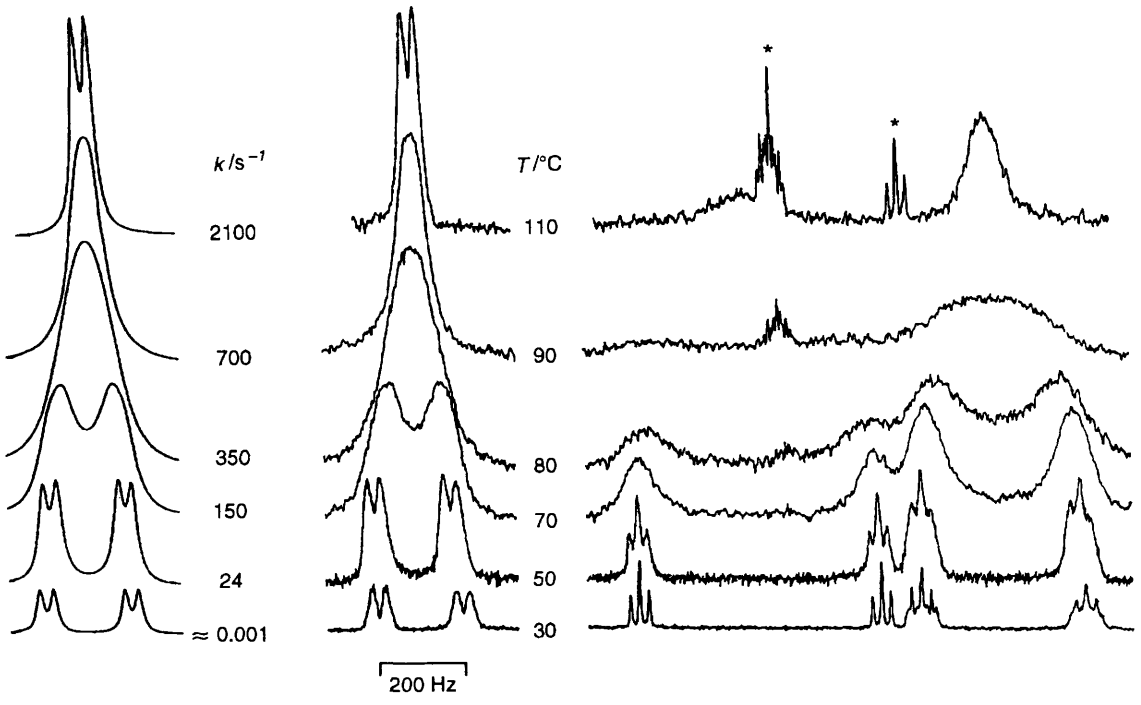

Fig. 4 The ^{19}F NMR spectra of $[Pd(C_6F_5)_2(terpy)]$ in $(CDCl_2)_2$ in the temperature range 30–110 °C. Computer-simulated spectra of the *o*-fluorine signals are shown on the left with 'best-fit' rate constants for the fluxional process. The asterisk indicates impurity signals

Table 6 Activation parameters for M–N fluxion in the complexes $[M(C_6F_5)_2(terpy)]$ (M = Pd or Pt)

Complex	T/°C	E_a/kJ mol^{-1}	$\log_{10}(A/s^{-1})$	$\Delta H^{\ddagger}$/kJ mol^{-1}	$\Delta S^{\ddagger}$/J K^{-1} mol^{-1}	$\Delta G^{\ddagger a}$/kJ mol^{-1}
$[Pd(C_6F_5)_2(terpy)]^b$	30–140[c]	75.7 ± 1.1	13.6 ± 0.2	72.8 ± 1.2	5.8 ± 3.3	71.0 ± 0.2
d	50–120[e]	77.0 ± 1.9	13.9 ± 0.3	74.1 ± 2.0	10.8 ± 5.5	70.9 ± 0.3
$[Pt(C_6F_5)_2(terpy)]^b$	100–140[f]	96.2 ± 2.9	13.2 ± 0.4	93.0 ± 2.9	−3.2 ± 7.3	93.9 ± 0.7

[a] At 298.15 K. [b] Values based on bandshape analysis of the exchanging signals AB ⇌ EF in the ^1H NMR spectra. [c] Static parameters measured at 0 °C. [d] Values based on bandshape analysis of the exchanging signals A(*o*,*m*) ⇌ B(*o*,*m*) in the ^{19}F NMR spectra. [e] Static parameters measured at 30 °C. [f] Static parameters measured at 70 °C.

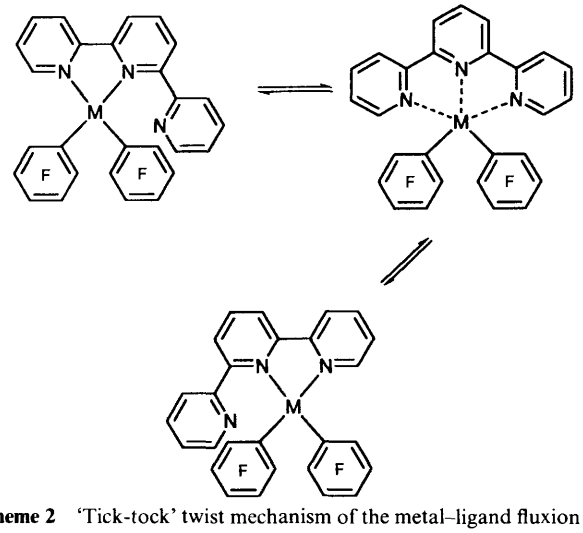

Scheme 2 'Tick-tock' twist mechanism of the metal–ligand fluxion

the equatorial ligands both in the ground and transition-state structures.

(*c*) *Below-ambient-temperature studies.* Such studies were undertaken in order to investigate any restricted rotations of the pendant pyridyl ring and the pentafluorophenyl rings.

^1H *NMR spectra.* The ^1H NMR spectra of both the palladium(II) and platinum(II) complexes in CD_2Cl_2 were essentially unchanged in the temperature range ambient to *ca.* −100 °C. This was rather unexpected and suggested that either ring rotations were always fast on the ^1H chemical shift timescale or the preferred rotamers were chemically indistinguishable and any exchange between them did not involve any detectable ^1H magnetisation transfer.

^{19}F *NMR spectra.* The ^{19}F NMR spectra of both complexes did, however, show significant changes on cooling below room temperature. All signals with the exception of the two triplets due to the *para*-ring fluorines broadened and then split into equal-intensity pairs. The case of the palladium(II) complex is shown in Fig. 5. The chemical shifts of the limiting low-temperature spectrum are shown in Table 4 together with similar data for the 'static' platinum(II) complex. These observations are indicative of restricted rotation of either both C_6F_5 rings, or the unco-ordinated pyridyl ring or all three rings. The fact that the *o*- and *m*-fluorine signals split into equal-intensity pairs and that there is no temperature effect on the *p*-fluorine signal implies that at the lowest temperatures, < *ca.* −50 °C, the complex exists in two chemically identical rotameric forms. Most likely structures are those where the planes of the C_6F_5 rings and the pendant C_5H_5N ring are mutually parallel and orthogonal to the plane of the co-ordinated bipyridyl portion of the ligand (Scheme 3).

The dynamics of the ring-rotation process(es) was probed by bandshape analysis of the *o*-fluorine signals. Spectra, recorded between ambient and −100 °C, revealed large chemical shift changes of the fluorine signals. These were measured directly from spectra in the range −100 to −50 °C and the shifts used in

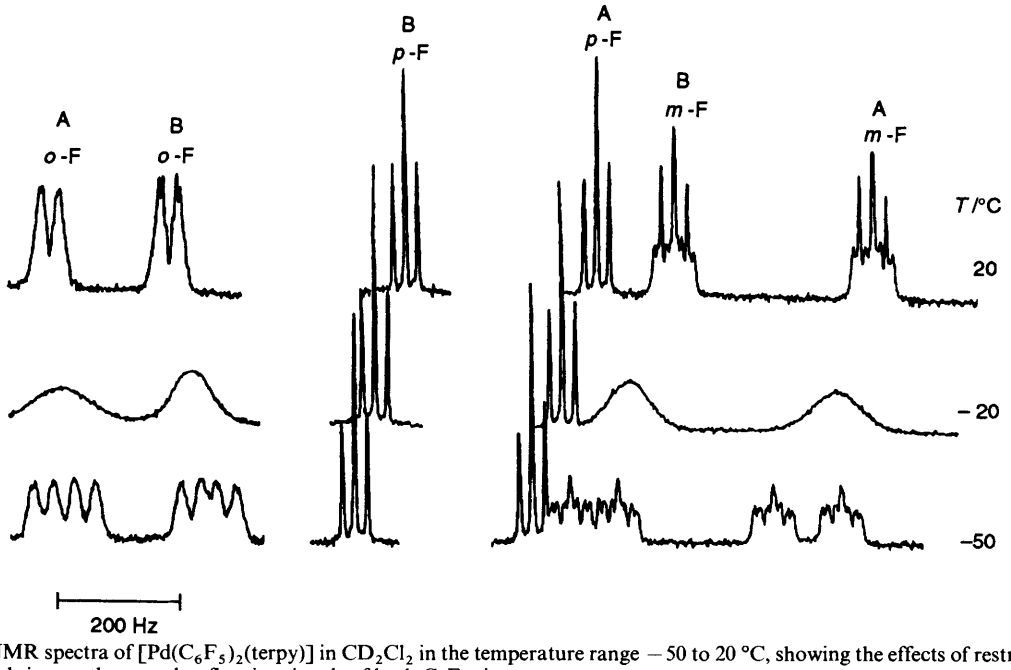

Fig. 5 The ^{19}F NMR spectra of $[Pd(C_6F_5)_2(terpy)]$ in CD_2Cl_2 in the temperature range −50 to 20 °C, showing the effects of restricted rotation of the pendant pyridyl ring on the *o*- and *m*-fluorine signals of both C_6F_5 rings

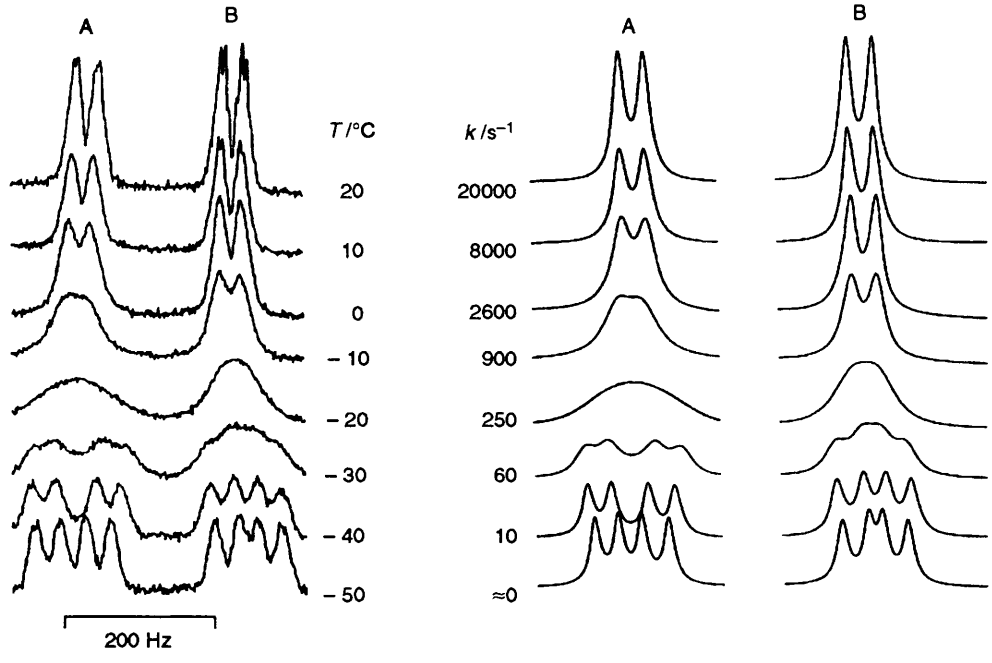

Fig. 6 The ^{19}F NMR spectra of the *o*-fluorine signals of $[Pd(C_6F_5)_2(terpy)]$ in CD_2Cl_2 in the temperature range −50 to 20 °C. Computer-simulated spectra with 'best-fit' rate constants are shown on the right

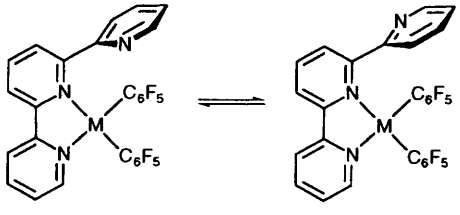

Scheme 3 Proposed solution rotamers of the complexes $[M(C_6F_5)_2(terpy)]$

the subsequent bandshape analysis in the higher-temperature range (−50 to 20 °C) were based on extrapolation of the lower-temperature values. Allowance was also made in this analysis for the three-bond *ortho–meta* fluorine couplings. Bandshape changes of the *o*-fluorine signals of ring A were simulated first, followed by the fittings of the ring B fluorine signals. Surprisingly, optimum fittings of both ring A and B signals were achieved with the *same* magnitude of rate constant (Fig. 6). Exactly the same outcome occurred for the fittings of the platinum(II), *o*-fluorine signals. From these fittings activation-energy data were calculated in the usual way (Table 7).

These energy values are significantly lower than values for the M–N fluxion. Magnitudes for the palladium(II) complex appear to be somewhat less reliable than those for the platinum(II) complex in view of the large associated $\Delta S^{\ddagger}$ value for the former (74.3 J K^{-1} mol^{-1}). This value is thought to be more suggestive of a small systematic error in the fittings rather

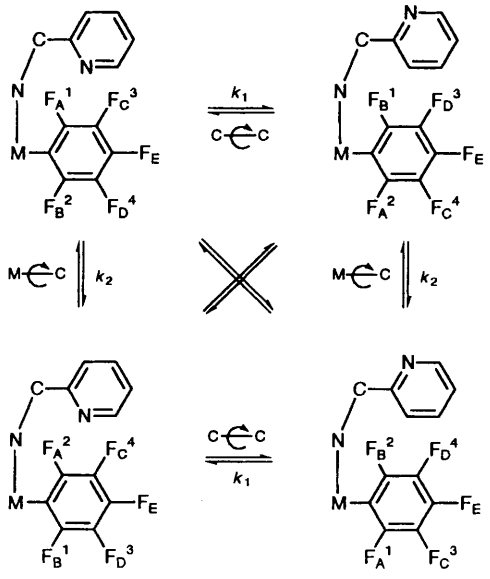

Scheme 4 Interconverting rotameric structures of the complexes $[M(C_6F_5)_2(terpy)]$ resulting from C–C (pyridyl) and M–C (C_6F_5) (ring A) rotations

Table 7 Activation parameters[a] for restricted ring rotation of the pendant pyridine ring in the complexes $[M(C_6F_5)_2(terpy)]$ (M = Pd or Pt)

Parameter	$[Pd(C_6F_5)_2(terpy)]$	$[Pt(C_6F_5)_2(terpy)]$
T/°C	−40 to 20[b]	−20 to 30[c]
E_a/kJ mol^{-1}	71.3 ± 1.4	57.7 ± 1.4
$\log_{10}(A/s^{-1})$	17.1 ± 0.3	13.1 ± 0.3
$\Delta H^{\ddagger}$/kJ mol^{-1}	69.1 ± 1.4	55.4 ± 1.5
$\Delta S^{\ddagger}$/J K^{-1} mol^{-1}	74.3 ± 5.5	−1.6 ± 5.5
$\Delta G^{\ddagger}$[d]/kJ mol^{-1}	47.0 ± 0.2	55.9 ± 0.2

[a] Values based on bandshape analysis of the exchanging signals $o,m \rightleftharpoons o',m'$ in the ^{19}F NMR spectra. [b] Static parameters measured at −50 °C. [c] Static parameters measured at −70 °C. [d] At 298.15 K.

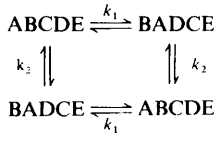

Scheme 5

than having any chemical significance. A lower $\Delta S^{\ddagger}$ value would produce an increased $\Delta G^{\ddagger}$ value for Pd^{II} and we are inclined to the view that the rate processes for both metal complexes have similar activation energies in the $\Delta G^{\ddagger}$ range of 47–56 kJ mol^{-1}.

We now need to consider carefully to which rate process(es) these activation energies refer.

Identification of the ring-rotation process. There are three potential bond-rotation processes to consider in the low-temperature NMR spectra of these *cis*-$[M(C_6F_5)_2(terpy)]$ (M = Pd^{II} or Pt^{II}) complexes, namely C–C rotation of the pendant pyridyl ring, M–C rotation of the C_6F_5 ring (A) and M–C rotation of the C_6F_5 ring (B). Initially, it was assumed that at ambient temperatures all three rotations would be fast on the ^{19}F chemical shift time-scale, but on cooling the rotations would become arrested. Considering first the rotations of the pyridyl ring and the adjacent C_6F_5 ring (arbitrarily labelled A). Such rotations cause exchange between the four partial structures shown in Scheme 4. Assuming that the planes of these two rings are closely parallel, then C–C rotation will exchange the *ortho* and *meta* ring fluorine pairs, A ⇌ B and C ⇌ D, with a rate constant k_1, and M–C rotation of C_6F_5 ring (A) will likewise produce mutual exchanges of these environments, with a rate constant k_2. Simultaneous rotation of both rings (represented by diagonal pathways in Scheme 4) will cause no nett effect and will be spectroscopically undetectable. The overall exchange problem is thus represented by Scheme 5 where the labels refer to Scheme 4. Since both types of rotation process cause the same chemical shift averaging then the NMR spectra will be sensitive only to the total or composite rate constant, $k_1 + k_2$, at any temperature. Now consider the rotation of the other C_6F_5 ring (B). Let us assume that this rotates with a rate constant k_3 at any temperature, in which case the fluorines of this ring will be sensitive to the total rate constant, $k_1 + k_3$. However, it was shown (*e.g.* Fig. 6) that the ^{19}F NMR spectra were sensitive to a *single magnitude* of rate constant, k, at any temperature. Thus, we have the relationship $k = k_1 + k_2 \approx k_1 + k_3$. Such a relationship could hold in three possible circumstances, namely (1) $k_1 = k_2 = k_3$, where these values fall within the NMR range of detection, (2) $k_1 \ll k_2$ or k_3, and $k_2 \approx k_3$, magnitudes of k_1 being too small for measurement, and (3) $k_1 \gg k_2$ or k_3, and $k_2 \neq k_3$ or $k_2 = k_3$, both k_2 and k_3 being too small for measurement. Case (1) is highly unlikely as it implies that the rates of rotation of the pyridyl ring and of both C_6F_5 rings are identical at any temperature. Rotation of the C_6F_5 ring adjacent to the pyridyl ring is likely to be far more restricted than rotation of the other ring. Case (2) implies that the spectra are sensitive only to the C_6F_5 ring rotations and that these occur at comparable rates, which, as stated above, is very unlikely. Furthermore it implies that the pyridyl ring is essentially locked or rotates slowly compared to C_6F_5 ring rotations at all measured temperatures. Case (3) suggests that the spectra are sensitive only to the pyridyl rotation, with rates of rotation of the C_6F_5 rings being slow compared to pyridyl rotation in the temperature range studied. This would seem to be the most plausible explanation of the observations. It allows for the likely possibility that both C_6F_5 rings may rotate at somewhat different rates and explains why the averagings of the *o*- and *m*-fluorine environments of *both* rings are sensitive to approximately the same magnitude of rate constant, k_1, namely that associated with the pyridyl ring rotation.

Our previous studies of octahedral metal complexes of terpy[1,3,4] have shown that low-temperature NMR spectra can detect restricted rotation of the unco-ordinated pyridine ring, so this present conclusion is compatible with earlier findings. For the present square-planar complexes of terpy, the rates of rotation of the C_6F_5 ligand rings are not measurable because of the dominating influence in the ^{19}F NMR spectra of the more rapid rotation of the unco-ordinated pyridyl ring at all temperatures above *ca.* −40 °C.

X-Ray Crystallography.—In order to confirm the bidentate chelate nature of terpyridine in the complexes in the solid state and to compare the structure with those of other bidentate terpyridine complexes the crystal structure of $[Pd(C_6F_5)_2(terpy)]$ was determined. Atomic fractional coordinates for $[Pd(C_6F_5)_2(terpy)]$ are given in Table 8. A view of the molecule indicating the numbering scheme adopted is shown in Fig. 7. The Pd atom has the expected square-planar co-ordination and the bidentate chelate nature of the terpyridine ligand is confirmed. This appears to be the first crystal structure obtained for a square-planar metal complex incorporating terpyridine co-ordinated in a bidentate fashion. Bond distances and selected bond angles are listed in Table 9.

The main distortions in the square-planar geometry around Pd arise from the small 'bite-angle' of terpyridine [N(1)–Pd–N(2) 77.9°]. The main distortions to the ligand on bidentate

Table 8 Atomic fractional coordinates ($\times 10^4$) for *cis*-[Pd(C_6F_5)$_2$(terpy)]

Atom	*x*	*y*	*z*	Atom	*x*	*y*	*z*
Pd	3 997(1)	7 537(1)	8 073(1)	C(18)	1 332(10)	6 305(6)	4 783(6)
N(1)	5 403(7)	7 916(4)	9 656(5)	C(19)	530(10)	7 156(6)	4 430(6)
N(2)	6 149(7)	8 835(4)	8 015(5)	C(20)	711(10)	8 081(6)	5 115(6)
N(3)	6 673(8)	7 381(6)	6 286(6)	C(21)	1 691(9)	8 138(5)	6 142(6)
C(1)	5 219(10)	7 319(6)	10 444(6)	C(22)	1 970(9)	6 443(5)	8 310(5)
C(2)	6 060(10)	7 716(6)	11 501(6)	C(23)	2 074(9)	5 369(5)	8 410(6)
C(3)	7 079(11)	8 740(7)	11 748(7)	C(24)	706(10)	4 618(5)	8 605(6)
C(4)	7 293(9)	9 369(6)	10 962(6)	C(25)	−897(10)	4 949(6)	8 668(6)
C(5)	6 441(8)	8 940(5)	9 900(5)	C(26)	−1 043(10)	6 020(7)	8 614(6)
C(6)	6 766(8)	9 468(6)	8 984(6)	C(27)	373(9)	6 740(6)	8 441(6)
C(7)	7 732(10)	10 542(6)	9 081(7)	F(17)	3 010(6)	5 530(3)	6 131(3)
C(8)	8 077(11)	10 934(7)	8 169(8)	F(18)	1 187(7)	5 394(4)	4 086(4)
C(9)	7 564(10)	10 255(6)	7 211(7)	F(19)	−382(7)	7 078(4)	3 404(4)
C(10)	6 636(9)	9 198(5)	7 174(6)	F(20)	−70(7)	8 904(4)	4 762(4)
C(11)	6 242(9)	8 413(6)	6 169(6)	F(21)	1 808(7)	9 094(3)	6 797(4)
C(12)	5 628(10)	8 719(6)	5 207(6)	F(23)	3 602(6)	4 994(3)	8 346(4)
C(13)	5 375(13)	7 995(8)	4 326(8)	F(24)	879(7)	3 572(4)	8 730(4)
C(14)	5 731(13)	6 965(9)	4 386(8)	F(25)	−2 250(7)	4 206(4)	8 825(5)
C(15)	6 422(11)	6 677(7)	5 370(8)	F(26)	−2 567(6)	6 347(5)	8 731(5)
C(16)	2 519(8)	7 332(5)	6 553(6)	F(27)	148(6)	7 795(3)	8 392(4)
C(17)	2 252(9)	6 398(5)	5 816(6)				

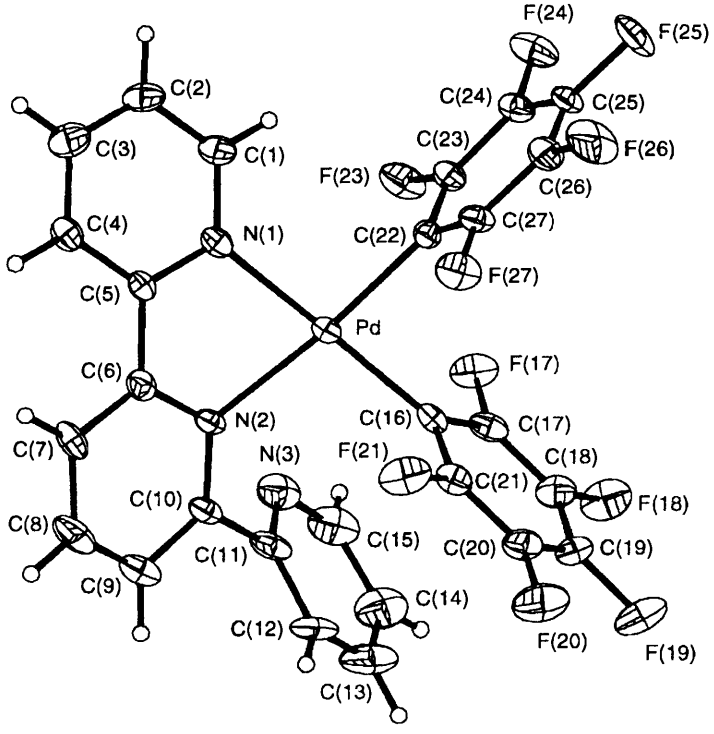

Fig. 7 A view of the crystal structure of [Pd(C_6F_5)$_2$(terpy)] showing the atom labelling

co-ordination occur at atoms N(1) and N(2) with bond angles C(1)–N(1)–C(5) and C(10)–N(2)–C(6) of 119 and 119.6° respectively compared with the corresponding angle of 116° at N(3) and an average bond angle at nitrogen of 116.2° in terpyridine.[21] The individual pyridine rings do not deviate significantly from planarity but the two co-ordinated rings are inclined to each other at an angle of 16° and the pendant ring is inclined at an angle of 46° to the adjacent co-ordinated ring, the dihedral angle N(2)–C(10)–C(11)–N(3) being −45.93°.

The Pd–N distances are unequal with Pd–N(2) 2.131 and Pd–N(1) 2.064 Å. This feature is also observed in the crystal structure of [ReBr(CO)$_3$(terpy)][3] and [PtIMe$_3$(terpy)].[4] In contrast to this the crystal structure of [Pd(OH)(terpy)]ClO_4·H_2O shows that when terpy is co-ordinated in a terdentate manner the Pd–N bond associated with the central pyridine ring is shorter than the Pd–N bonds to the outer rings.[22]

The pentafluorophenyl groups are distorted from regular hexagons, mainly at the *ipso*-carbon atoms with values of 113 and 115° for the angles C(17)–C(16)–C(21) and C(23)–C(22)–C(27) respectively. The C_6F_5 ring (A), is inclined at an angle of 13° to the plane of the adjacent unco-ordinated pyridine ring, the shortest non-bonded distance between the two rings being 3.13 Å for C(11)···C(16). The absolute orientation of this C_6F_5 ring may be expressed in terms of the dihedral angles N(2)–Pd–C(16)–C(17) (113.72°) and N(2)–Pd–C(16)–C(21) (−65.03°). The other C_6F_5 ring (B) is rotated about 90° with respect to the adjacent co-ordinated pyridine ring, the dihedral angles in this case being N(1)–Pd–C(22)–C(23) (−82.49°) and N(1)–Pd–C(22)–C(27) (94.12°).

For the purposes of interpreting the results of the low-temperature solution ^{19}F NMR studies it was necessary to postulate that, at low temperatures, the unco-ordinated

Table 9 Bond lengths (Å) and selected angles (°) for [Pd-$(C_6F_5)_2$(terpy)]

Pd–N(1)	2.064(6)	Pd–N(2)	2.131(5)
Pd–C(16)	2.011(7)	Pd–C(22)	1.994(7)
N(1)–C(1)	1.336(9)	N(1)–C(5)	1.349(8)
N(2)–C(10)	1.325(8)	N(2)–C(6)	1.358(9)
N(3)–C(15)	1.362(11)	N(3)–C(11)	1.388(9)
C(1)–C(2)	1.381(10)	C(2)–C(3)	1.344(11)
C(3)–C(4)	1.362(11)	C(4)–C(5)	1.397(10)
C(5)–C(6)	1.459(9)	C(6)–C(7)	1.392(9)
C(7)–C(8)	1.384(1)	C(8)–C(9)	1.370(12)
C(9)–C(10)	1.376(9)	C(10)–C(11)	1.491(11)
C(11)–C(12)	1.345(10)	C(12)–C(13)	1.342(12)
C(13)–C(14)	1.355(12)	C(14)–C(15)	1.372(12)
C(16)–C(21)	1.361(9)	C(16)–C(17)	1.386(10)
C(17)–C(18)	1.351(10)	C(17)–F(17)	1.360(7)
C(18)–F(18)	1.352(8)	C(18)–C(19)	1.374(10)
C(19)–F(19)	1.344(8)	C(19)–C(20)	1.351(10)
C(20)–F(20)	1.334(8)	C(20)–C(21)	1.364(10)
C(21)–F(21)	1.370(8)	C(22)–C(23)	1.363(9)
C(22)–C(27)	1.388(9)	C(23)–F(23)	1.357(8)
C(23)–C(24)	1.373(9)	C(24)–F(24)	1.346(8)
C(24)–C(25)	1.387(10)	C(25)–F(25)	1.339(8)
C(25)–C(26)	1.358(11)	C(26)–F(26)	1.345(9)
C(26)–C(27)	1.366(10)	C(27)–F(27)	1.352(8)
C(22)–Pd–C(16)	85.2(3)	C(22)–Pd–N(1)	96.1(2)
C(16)–Pd–N(1)	173.3(2)	C(22)–Pd–N(2)	172.2(2)
C(16)–Pd–N(2)	100.3(2)	N(1)–Pd–N(2)	77.9(2)
C(5)–N(1)–Pd	113.6(4)	C(1)–N(1)–Pd	126.9(5)
C(1)–N(1)–C(5)	119.0(6)	C(10)–N(2)–C(6)	119.6(6)
C(10)–N(2)–Pd	129.3(5)	C(6)–N(2)–Pd	109.4(4)
C(15)–N(3)–C(11)	116.6(7)	C(23)–C(22)–C(27)	115.0(6)
C(21)–C(16)–C(17)	113.0(7)	N(2)–C(10)–C(11)	118.7(6)
N(1)–C(5)–C(6)	115.1(6)	C(12)–C(11)–N(3)	122.3(7)
N(2)–C(6)–C(5)	116.3(6)	N(3)–C(11)–C(10)	115.8(7)
C(12)–C(11)–C(10)	121.7(6)		

pyridine was orthogonal to the adjacent co-ordinated ring and parallel to the two C_6F_5 rings, with the three rings adopting an orientation perpendicular to the N(1)–N(2)–C(16)–C(22) plane. This is clearly not the structure observed in the solid state. The fact that the orientations of the rings differ significantly from the averaged orientations in solution is probably because of molecular packing constraints in the solid state.

Acknowledgements

We are grateful to the SERC for a studentship (to H. M. P.).

References

1 Part 3, E. W. Abel, K. G. Orrell, A. G. Osborne, H. M. Pain and V. Šik, *J. Chem. Soc., Dalton Trans.*, 1994, 111.
2 E. C. Constable, *Adv. Inorg. Chem. Radiochem.*, 1986, **30**, 69.
3 E. W. Abel, V. S. Dimitrov, N. J. Long, K. G. Orrell, A. G. Osborne, H. M. Pain, V. Šik, M. B. Hursthouse and M. A. Mazid, *J. Chem. Soc., Dalton Trans.*, 1993, 597.
4 E. W. Abel, V. S. Dimitrov, N. J. Long, K. G. Orrell, A. G. Osborne, V. Šik, M. B. Hursthouse and M. A. Mazid, *J. Chem. Soc., Dalton Trans.*, 1993, 291.
5 G. Lopez and G. Garcia, *Inorg. Chim. Acta*, 1981, **52**, 87.
6 G. Lopez, G. Garcia, N. Cutillas and J. Ruiz, *J. Organomet. Chem.*, 1983, **241**, 269
7 D. F. Shriver, *Manipulation of Air-sensitive Compounds*, McGraw-Hill, New York, 1969.
8 D. A. Kleier and G. Binsch, DNMR 3, Program 165, Quantum Chemistry Program Exchange, Indiana University, IN, 1970.
9 V. Šik, Ph.D. Thesis, University of Exeter, 1979.
10 A. A. Danopoulos, M. B. Hursthouse, B. Hussain-Bates and G. Wilkinson, *J. Chem. Soc., Dalton Trans.*, 1991, 1855.
11 G. M. Sheldrick, SHELX 76, Program for Crystal Structure Determination and Refinement, University of Cambridge, 1976; DIFABS, N. P. C. Walker and D. Stuart, *Acta Crystallogr., Sect. A*, 1983, **39**, 158.
12 R. Usón and J. Forniés, *Adv. Organomet. Chem.*, 1988, **28**, 219.
13 E. Maslowsky, jun., *Vibrational Spectra of Organometallic Compounds*, Wiley, New York, 1977.
14 R. J. Abraham, *The Analysis of High Resolution NMR Spectra*, Elsevier, Amsterdam, 1971, ch. 3.
15 H. Kessler, M. Gehrke and C. Griesinger, *Angew. Chem., Int. Ed. Engl.*, 1988, **27**, 490.
16 R. Usón, J. Forniés, M. Tomás, B. Menjón, C. Fortuño, A. J. Welch and D. E. Smith, *J. Chem. Soc., Dalton Trans.*, 1993, 275.
17 R. Usón, J. Forniés, M. A. Usón and S. Herrero, *J. Organomet. Chem.*, 1993, **447**, 137.
18 E. R. Civitello, P. S. Dragovich, T. B. Karpishin, S. G. Novick, G. Bierach, J. F. O'Connell and T. D. Westmoreland, *Inorg. Chem.*, 1993, **32**, 237.
19 J. B. Brandon, M. Collins and K. R. Dixon, *Can. J. Chem.*, 1987, **56**, 950.
20 E. W. Abel, S. K. Bhargava and K. G. Orrell, *Prog. Inorg. Chem.*, 1984, **32**, 1.
21 C. A. Bessel, R. F. See, D. L. Jameson, M. R. Churchill and K. J. Takeuchi, *J. Chem. Soc., Dalton Trans.*, 1992, 3223.
22 P. Castan, F. Dahan, S. Wimmer and F. L. Wimmer, *J. Chem. Soc., Dalton Trans.*, 1990, 2679.

Received 15*th July* 1994; *Paper* 4/04338C